OPTOACOUSTIC EFFECTS IN AEROSOLS

N.N. Bochkarev, N.P. Krasnenko, and Yu.M. Sorokin

Institute of Atmospheric Optics,
Siberian Branch of the Academy of Sciences of the USSR, Tomsk
Received January 10, 1990

Experimental and theoretical works on the problem of laser generation of acoustic -waves in atmospheric aerosol are reviewed.

A number of effects arising in the case of solid- and liquid-state aerosol below and above the threshold for the development of an optical discharge produced by the interaction with the radiation are examined. A classification of the acoustic waves that arise is given. The possibilities of remote optoacoustic diagnostics of the parameters of laser radiation and aerosol are analyzed.

1. INTRODUCTION

Optoacoustic effects produced in aerosols, as a rule, by rapid and nonuniform heating of two-phase systems above and below the threshold for the development of an optical discharge, produced by the interaction with radiation, form am entire class of physical processes which have become very important in the last few years in connection with the applications of high-power laser radiation. Until recently there was no general theory of the generation of acoustic waves (AWs) by such radiation in aerodispersed systems. The thermal mechanism ("photoacoustic effect" — see Ref. 1) of the generation of AWs in an atmosphere containing aerosol particles is examined in Ref. 2. A brief review of pre-1985, primarily experimental, works on laser generation of AWs accompanying optical breakdown in atmospheric aerosol is given in Ref. 3.

The significant progress made in this field in the last few years is attributable to the accumulation of experimental data and improvement of methods for processing them, extension of the spectral interval of the measurements into the ultrasonic region, development of methods for numerical modeling of AWs, observation of the generation of AWs under subthreshold conditions, and development of models of the generation of hypersonic and sonic AWs, including in the case of low-threshold collective optical plasma formation. As a result it is possible to propose a systematic theoretical picture of laser generation of AWs in aerosols in a wide range of values of the parameters, to give a classification of the AWs which arise in both the subthreshold regime and in optical discharges of different types, and to analyze, based on this, the existing possibilities for remote optoacoustic diagnostics. The purpose of this review is, in addition to giving a brief systematization of the numerical results and experimental data on laser generation of AWs in aerosol, to examine the questions enumerated above.

The generation of AWs under subthreshold conditions accompanying vaporization of a water atmospheric aerosol ("photohydraulic effect" — see Ref. 5) by pulsed radiation ($\lambda = 10.6$ μm, $W_p \sim 100$ J, and $\tau_1 \sim 1$ μsec) was observed in Ref. 4 and later investigated in Refs. 6–8 for a model water aerosol. Primarily the dependences of the peak values of the acoustic pressure on the energy density of the laser pulse and the concentration of water-aerosol particles (liquld-water content of the aerosol) were determinated. An estimate of the conversion factor, characterizing the conversion of the laser-energy absorbed per unit volume into acoustic energy, $K_{AW} \sim 10^{-7}$ accompanying the propagation of a laser pulse in the atmosphere shows that the average intensity of the AWs is high enough in order to record reliably a signal at a distance of the order of 1 km using directional acoustic detectors.

The optoacoustic effects accompanying the development of plasma foci (PF) on isolated solid aerosol particles in air have been studied in much greater detail.[9–15] The systematic study of the spectral and energy characteristics of AWs generated by the entire aggregate of interacting PF was Initiated by Belyaev et all.[9,10] Their measurements of the acoustic pressure generated by discharges of the type long laser spark (LLS) led to an estimate of the acoustic energy released in a single plasma focus ($W_{PF} = 10^{-8}$–10^{-3} J), and the results of spectral analysis of AWs from the acoustic range made it possible to associate the minima in the spectra of AWs with the length of the discharge and the characteristic distance between separate plasma foci.

Time-resolved acoustic signals from separate plasma foci[11,13] made it possible to relate their width $\tau_s \sim 10^{-4}$ sec and the amplitude with the size of the plasma focus for sufficiently short laser pulses ($\tau_1 \leq \tau_s$) as well as to make a more accurate estimate of the conversion factor, characterizing the conversion of the laser energy absorbed by the plasma focus

0235-6880/90/06 513-15 $02.00

into acoustic energy ($K_{AW} \sim 10^{-4}$). It was possible to reconstruct from the optoacoustic measurements the critical sizes of the breakdown-initiating aerosol particles as a function of the energy density of the laser radiation; this is of interest for predicting the propagation of high-power beams on atmospheric paths. The numerical modeling of AWs generated by a discharge of the LLS type, as a random sequence of square pulses whose parameters (width, amplitude, and repetition interval) are uniformly distributed on some interval[14] made it possible to make a well-founded determination of the character of the interaction between the position of the minima in the frequency spectrum of the AWs and the average distance between separate plasma foci. In the process, the correlation, following from the results of Refs. 11 and 13, between the position of the high-frequency maximum in the frequency spectrum of the LLS ($f \simeq 3$ kHz) and the diameter of the plasma focus $d_{PF} \simeq v_s(2\pi f)^{-1} \simeq 2$ cm, where v_s is the velocity of sound, was confirmed. The mutually complimentary nature of the information from acoustic and optical signals from LLS and, in this connection, the potential usefulness of combined optoacoustic diagnostics of discharges was pointed out by Geints et al. in Ref. 15.

From the standpoint of the diversity of the physical mechanisms for generation of AWs the richest discharge is a collective optical discharge (COD), which arises in dense aerodispersed media at minimum intensities in a field generated by sufficiently long pulses. A collective optical discharge is formed and develops primarily by means of a heat-conduction mechanism without the formation of photodetonation waves of absorption of laser radiation which are characteristic for the dynamics of plasma foci in discharges of the LLS type. Nonetheless, as was first pointed in Ref. 16, even this discharge is a source of intense AWs. In Ref. 17 it was stated that the acoustic spectrum of the COD contains a relative maximum at $f \sim 10^{14}$ Hz.

A complete investigation[18–20] of the dynamics of acoustic disturbances generated by the region of the COD in a solid-state aerosol made it possible to prove that here there exist acoustic components of at least two forms: internal hypersonic waves with maximum frequencies $f_{max} \sim 1$—10 MHz and outgoing waves with characteristic frequencies $f \sim 1$—10 kHz.

Analysis of the numerical results[18–19] and laboratory experiments[18,20] showed that the characteristics of the generation of some hypersonic components of AWs in a solid-state aerosol are similar for both CODs and discharges of other types. The approach to estimating the spectral intervals of generation of separate low-frequency components of AWs for different optical discharges is also analogous. This creates a basis for constructing a quite general classification of AWs generated by laser radiation in, at least, a solid-state aerosol.

2. NEAR-FIELD HYPERSONIC DISTURBANCES

The starting point for the construction of a picture of the generation and evolution of AWs in a solid-state aerosol under the action of not-too-short laser pulses ($\tau_1 \gtrsim 10$ sec) is the idea of the formation of a vapor-air aureole (VAA) in the vicinity of a rapidly evaporating particle; the transition of this aureole with significant heating into a vapor-plasma microflame is possible only when some threshold conditions are satisfied. Irrespective of whether or not the threshold has been exceeded, the AWs generated in the system can be divided into two types: internal or near-field hypersonic waves, which, because of strong damping, can be studied primarily by numerical methods only, and external sound waves recorded by acoustic sensors at different distances from the region of laser-aerosol interaction. It has been found that, on the contrary, numerical methods are not effective for describing the latter type of waves.

A numerical model of the generation of near-field AWs should make it possible to trace the transformation of the vapor-air aureole surrounding a particle into a microplasma focus (microflame), i.e., the model should describe both below- and above-threshold regimes for an optical discharge. To make a quantitative calculation of the spatiotemporal structure of such a system it is necessary to employ a mathematical model that gives a self-consistent description of the heating of a particle and vaporization in a layer near the particle as well as the dynamics of the interaction of the components in the entire aureole (which, under the conditions of volume energy release, is expanding) and takes into account the real temperature dependences of the thermophysical and gas-dynamic parameters of the vapor-air mixture. Such a model was constructed in Refs. 18 and 19.

Analysis of the results of numerical modeling of the dynamics of VAA in a quite wide range of intensities $I = (4\text{—}400) \cdot 10^6$ W/cm^2 shows that there are three basic stages: initial, convective, and heat-conducting. The starting stage includes heating of the particle and establishment of a regime of developed vaporization, accompanied by the formation of a pressure shock. The convective stage corresponds to three-dimensional expansion of VAA under the backpressure exerted by the air. The work performed by the vapor against the air pressure under conditions when the air is almost completely forced out of the inner regions of the VAA ("piston"), as well as the absorption of laser energy by the vapors results in heating of the prefrontal zone. In the case when the velocity of the front is high (of the order of v_s), however, the convective mechanism plays the main role in the redistribution of heat and vapor and significant heating of the VAA does not occur.

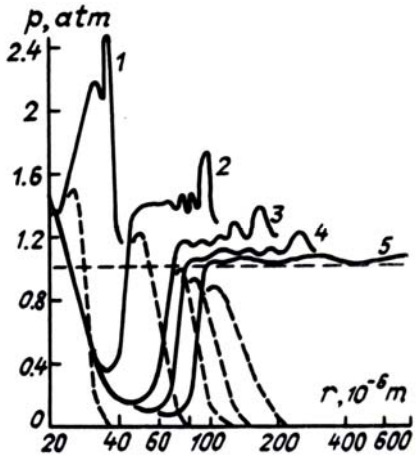

FIG. 1. An acoustic wave of aureole formation (AWF) on a corundum particle with radius $a = 20$ μm *and volume absorption coefficient* $\alpha = 5 \cdot 10^3$ cm^{-1} *with intensity* $I = 4 \cdot 10^6$ W/cm^2 *at successive moments in time* (μsec)*:* 0.16 *(1),* 0.33 *(2),* 0.57 *(3),* 0.92 *(4), and* 2.86 *(5): The dashed lines show the profiles of the partial pressure of the aerosol vapors. The absorption coefficient of the vapor-air aureole at the wavelength of the neodymium laser* $\mu(T)$ *was calculated using the formulas from Ref. 21. The difference between the absorption coefficient* α *and the linear value (the "aerosol blackening" effect), following from the results of Ref. 22, is taken into account.*

Hypersonic AWs, arising already at the initial stage of the evolution of a VAA (curves 1 and 2 in Fig. 1), are characterized by frequencies right up to $f \sim 10^8$ Hz. At the convective stage their amplitude decreases rapidly and this process is accompanied by a shift of the spectrum to lower frequencies (down to $f \sim 10^6$ Hz over a time $\Delta t \sim 3$ μsec), as one can see from Fig. 1 (see curves 3–5).

The process proceeds under conditions such that nonlinearity competes with high-frequency dissipation accompanied by three-dimensional spherical expansion of VAA. The associated acoustic waves can be called an acoustic wave of aureole formation (AWF). We note that the velocity of the wave displacing the buffer gas drops rapidly (from 200 m/sec to 40 m/sec over a time $\Delta t \sim 3$ μsec), so that the AWF is detached from it and the zone of heating and already propagates in a cold buffer gas. The amplitude of the AWF at a distance $r \sim 1$ mm with $f \sim 1$ MHz is $\Delta P_1 \sim 0.02$ atm. The further evolution of the AWF and the possibility of remote detection of the wave are determined primarily by the linear absorption with the coefficient $\alpha_s = 2\pi^2\nu f^2/(v_s\rho_a) \leq 0.6$ cm^{-1} and the geometric factor r^{-1}, where ν is the coefficient of kinematic viscosity and is the air density.

The velocity of the medium at the point of maximum temperature drops monotonically during the convective stage of development of the VAA. The transition from the convection to the heat-conducting stage of the evolution of the VAA occurs when the rate of convection is equal to the rate of heat conduction in the indicated region and corresponds to separation of two spatial regions in the three-dimensionally expanding aureole: an inner, comparatively stable, region in which convection plays the main role as before and an outer region (which determines the maximum size and temperature of the VAA), in which heat conduction predominates and the pressure is close to atmospheric pressure. It follows from what was said above that in the absence of significant heating of the VAA (i.e., in the subbreakdown regime) new components of AWs of an isolated aerosol particle are not generated. It is this regime that is illustrated in Figs. 1 and 2; in addition, Fig. 2 corresponds to the moment of virtually complete vaporization of the aerosol particle (ζ is a generalized parameter).

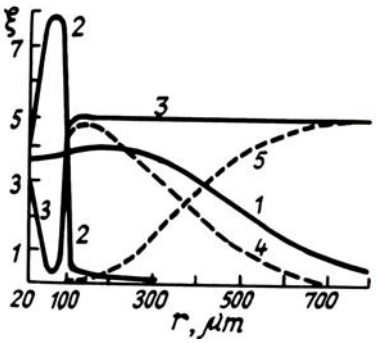

FIG. 2. The heat-conducting stage of the evolution of a vapor-air aureole (VAA) in the subbreakdown regime. Profiles: 1) the temperature $T = 10^3\xi$ K*; 2) the velocity* $V = 2 \cdot 10^2\xi$ m/sec*; 3) the total pressure* $P = 0.2\xi$ atm*; 4) the partial pressure of the aerosol vapors; 5) the partial pressure of the buffer gas. The conditions are the same as in Fig. 1. The time* $t = 43.6$ μsec*. The relative mass of the vaporized aerosol* $m_a/m_0 \simeq 1$.

The specific nature of the interaction of high-power laser radiation of subbreakdown intensity with a water aerosol is connected primarily with the focusing and explosion of particles or ejection of jets with comparatively low temperature from the particles and does not qualitatively change the physical mechanism of generation of AWFs as a process in which the pressure shocks decay on the front of the VAA. Essentially, only the geometry of the VAA front changes. This means that at distances much larger than the radius of the particle ($r \geq a$) it should be expected that the AWF should have the same asymptotic behavior for both solid-state and water aerosols.

3. ACOUSTIC DISTURBANCES IN THE FAR FIELD

The possibility of remote detection of subbreakdown acoustic waves is connected primarily with the

transformation of the spectrum of hypersonic AWFs owing to HF dissipation and dispersion[23] into the low-frequency (acoustic) range, where the linear absorption coefficient $\alpha_s \sim f^2$ is quite small.

The thermal and evaporation mechanism of sound generation in continuous media as well as the formation of AWs in the far field have been examined in detail in a number of works (see, for example, Refs. 1 and 24 and the references cited therein). We discuss below the results of works on the investigation of the generation of AWs by the natural atmospheric and model mono- and polydispersed water aerosols under the action of pulsed CO_2-laser radiation.[4,6–8] A monodispersed aerosol, generated by an ultrasonic generator. Is a convenient model for studying the processes occurring when a separate aerosol particle breaks up in the field of high-power laser radiation. The acoustic waves recorded in the far zone in this case consist of contributions from AWs generated by separate particles. The width of the acoustic signal in the far zone for short laser pulses ($\tau_s \le v_s \cdot 2R$, where R is the radius of the laser beam) is determined by the volume of the region of laser-aerosol interaction, and its amplitude is proportional to the amplitude of the acoustic wave generated by separate particles (for monodispersed aerosol it is proportional to the concentration of aerosol particles; this has been quantitatively verified in Ref. 7).

The dependence of the acoustic pressure p in the far zone on the energy density of the laser radiation (Fig. 3) indicates that this dependence changes much more rapidly for a monodispersed aerosol after the threshold of explosive boiling of the aerosol particles is reached ($E_{\text{exp}} \simeq 2$ J/cm^2).[7,8] For $E_1 < E_{\text{exp}}$, however, no difference was observed in the behavior of the dependences $P(E_1)$ for poly- and mono-dispersed aerosols: as E_1 increases the linear dependence transforms continuously into a quadratic dependence.

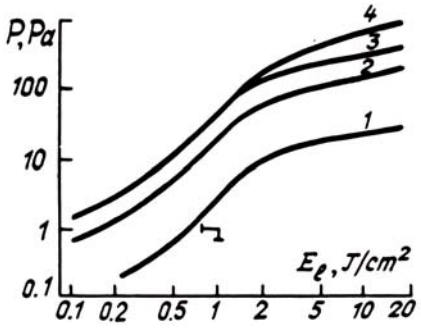

*FIG. 3. The acoustic pressure generated in the far zone (*5 cm *from, the center of the interaction volume) by a monodispersed aerosol (1–3) and a polydispersed aerosol (4) as a function of the energy density of pulsed CO_2-laser radiation for initial liquid-water content of the aerosol* (g/m^3): 8 *(1),* 40 *(2),* 80 *(3), and* 800 *(4).*

References 7 and 8 contain data on the saturation of the acoustic pressure as the initial liquid-water content of the aerosol increases while the energy density of the laser radiation remains fixed. This is connected with the effective penetration depth of the laser radiation into the aerosol cloud. Saturation occurred with an initial liquid-water content of ~ 120 g/m^3.

Based on models of the dynamics of a phase explosion in water particles,[25] the increment to the temperature of the medium is determined from analysis of the heat stored in the products of explosion up to the moment at which they stop under the condition of thermodynamic equilibrium in the medium. Then the excess pressure ΔP in the region of interaction of the radiation with the aerosol can be found from the equation of state of the two-component air-vapor mixture[8]:

$$\Delta P \simeq \Delta\rho_v \left[R_v T_0 + \frac{C_{pv}}{C_{pa}} R_a (T_{v0} - T_0) \right], \quad (1)$$

where ρ_v, R_a, and R_v are, respectively, the density of the vapor and the gas constants of air and the vapor; C_{pv} and C_{pa} are the specific heat capacities of the vapor and air at constant pressure; T_{y0} is the initial temperature of the medium; and, T_{v0} is the temperature of the vapor up to the moment that the products of the explosion stop ($T_{v0} \simeq 373$ K). The increment to the density of water vapors in the interaction volume cam be expressed in terms of the total degree of evaporation of a separate aerosol particle $\Delta\rho_v = X_e q_0$, which is determined by the ratio of the liquid-water content of the fog at the end of and prior to the action of the radiation pulse: $X_e = 1 - q/q_0$.

For uniformly absorbing particles ($a \lesssim 10$ μm, $\lambda = 10.6$ μm) the degree of vaporization is virtually independent of the particle size, and is determined entirely by the energy parameters of the radiation pulse.[28] The presence of a coarse fraction ($a \gtrsim 10$ μm) of significant size in the aerosol, like in the case of the polydispersed fog employed in the experiments of Ref. 8, can substantially change the power parameters of the generated acoustic pulse. Since in large particles the heating is nonuniform, explosive boiling does not occur in the entire volume of the drop, like in small particles, but rather only in a surface layer, whose thickness is of the order of the absorption length of the radiation in water. It is easy to show that for am increment $\Delta\rho_v$ after the explosion of a polydispersed aerosol $\Delta\rho_v = 0.4 X_e \cdot q_0$.[8] Thus the acoustic disturbance accompanying the explosion of a fine-drop aerosol is approximately 2.5 times stronger than in the case of a polydispersed fog with a coarse fraction (assuming that they both contain the same amount of liquid water).

4. ACOUSTIC DISTURBANCES AT THE BREAKDOWN FOCUS

A microplasma focus (MPF) can form on an isolated particle by several different mechanisms, depending on the size and material of the aerosol parti-

cles as well as the width of the laser pulse. The best known mechanism is the comparatively high-threshold (with respect to the intensity) mechanism of thermal explosion of solid micron-size particles[27] followed by the development of an avalanche in an expanding, thermally weakly ionized VAA. This mechanism agrees well with the frequency dependence of the thresholds for breakdown of the coarse fraction of naturally dry atmospheric aerosol in discharges of the LLS type[28] with pulse widths $\tau_1 = 10^{-8}$–10^{-6} sec. Since in this case the intensities are, as a rule, high enough for a photodetonation wave (PDW) to be maintained in the buffer gas, the generation of AWs in the form of AWFs is replaced almost immediately by generation of a much more powerful AW whose spatial structure and spectrum are similar. The duration of this AW is now determined not by the characteristic formation time of the VAA, like in the case of AWF, but rather by the width of the laser pulse τ_1. This AW is connected with the motion of the heating front of the MPF and the propagation of PDW and can be called an acoustic wave of heating (AWH). An analogous picture should also be observed when the MPF is produced by different but quite rapid mechanisms (for example, focusing and multiphoton ionization in the case of a water aerosol[29]). The separation of the AWF and AWH, in this case, is quite arbitrary, especially since under conditions of external focusing of the radiation by the water aerosol[30] the stage of AWF in its pure form could be absent entirely.

A different situation arises for comparatively large particles ($a > 10$ μm) in the radiation field of wide near-IR pulses ($\tau_1 \gtrsim 10$ μsec), when under conditions of moderate absorption in the VAA self-maintained heating of the aureole is possible in the heat-conducting regime with low intensity, while generation of AWF and AWH is separated by a time interval of the order of 10 μsec. The dynamics of this process can be investigated numerically based on the mathematical model described in Refs. 18 and 19. Analysis shows[19] that above-threshold VAA evolves through the same stages as in the below-threshold regime (initial, convection, and heat-conduction). Significant differences from the behavior discussed in Sec. 2 appear only at the third stage, when at some critical time τ_* the heating in the vapor component of the VAA can exceed the losses (owing to heat conduction and diffusion expansion of the vapors). The maximum rate of heating of the VAA occurs in a narrow temperature range ($T \sim 7 \cdot 10^3$ K), corresponding to the position of the first maximum of the temperature dependence of the absorption coefficient $\mu(T)$ of the radiation initiating breakdown at the wavelength for aerosol vapors (see Ref. 21).

Figure 4 makes it possible to follow the dynamics of the VAA in the case of above-threshold (for heating) radiation intensity. In this case, in order to determinate more accurately the mechanism by which the VAA is heated the same value of the flow of the aerosol vapors from the particles (determined by the product $\alpha(I)$ as that in Figs. 1 and 2 was chosen.

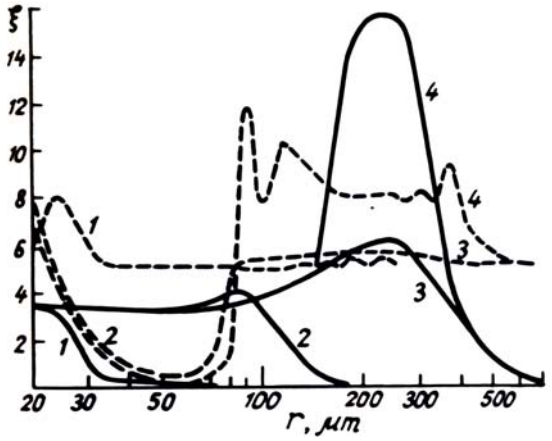

FIG. 4. The heat-conduct ion transformation of the vapor-air aureole (VAA) at the microplasma focus (MPF) in the above-threshold regime. The profiles of the temperature (solid lines) and pressure (dashed lines) are presented for the following times (μsec): 0.13 *(1),* 0.92 *(2),* 26 *(3), and* 26.3 *(4). The process of generation of acoustic waves of aureole formation (AWF) (1, 2) and acoustic waves of heating (AWH) (3, 4) at an aerosol particle with,* a = 20 μm *and* $\alpha = 50$ cm^{-1} *is followed for* $I = 4 \cdot 10^8$ W/cm^2 *in the following scale;* $T(K) = 10^3\xi$ *and* PI10^5Pa] = 0.2ξ.

As one can see from Fig. 4, the qualitative features of the heat-conduct ion stage of the development of VAA are preserved at the initial stage of heating. In contrast to the case of "cold" VAA, however, here the gas-dynamic regime is replaced with a delay of about 25 μsec; the distinguishing indicator of this process is rapid (over a time of the order of 10^{-7} sec) heating and therefore increase of the pressure, resulting in intensification of convection processes in the outer part of the VAA (Fig. 4). This stage of the development of a VAA can be called the convection-heat-conduction stage. Rapid growth of the maximum electron density N_e (from $(5–6) \cdot 10^{15}$ cm^{-3} to $1.5 \cdot (10^{17}–10^{18})$ cm^{-3} in Fig. 4) permits talking about transformation of VAA into MPF, by means of heat conduction, over a time of the order of 10^{-5} sec, which depends on the intensity of the incident radiation I and the size a and absorption coefficient α of the aerosol particle. Another consequence of the rapid increase in the temperature and pressure is that strong AWs, which are in many ways analogous to the waves generated at the initial stage of the evolution of the VAA, appear at the convection-heat-conduct ion stage of the development of an MPF. The most significant physical difference between them is that the zone of generation of AWs in the heated MPF is located at a distance $r_* \gg a$, far from the surface of the particle, and the AWH arising here travel from the zone of heating not only to the outside, but also into the particle. Their "collapse" to the particle is, however,

prevented by the supersonic gas flow in the interior convection region of the MPF. The interaction of the AWF with the flow results in compression of the convection region, rapid growth of the pressure at the boundary of the convection region with the heat-conduction region, and a unique reflection (reverberation) of the AWH, which increases the lifetime of AWH in the case of external detection.

The increase in the absorption coefficient of a particle with the same intensity (i.e., increase in the flux density of aerosol vapors) results in approximately a proportional reduction in the time during which the VAA is transformed by means of heat conduction into an MPF, i.e., the interval between the pulses of AWF and AWH decreases. This opens up definite possibilities for active acoustic diagnostics of the composition of aerosol particles.

The increase in the size of an aerosol particle under otherwise equal conditions results in an increases of the radius r_* of the zone of heating. The threshold intensity decreases ($\alpha Ia \simeq$ const), while the heating time increases. The duration of the generation of the AWF also increases. Thus there are definite prospects for performing diagnostics of the sizes of aerosol particles not only based on the energetics but also based on the temporal characteristics of the AWs.

The evolution of the MPF over a time determined by the width of the laser pulse or on spatial scales determined by the dimensions of the focal region, i.e., their transformation into the experimentally recorded plasma foci, is connected with the emergence of the plasma-format ion process into the buffer gas, for example, in the form of a photodetonation wave (for discharges of the LLS type), or with the development of collective mechanisms in an ensemble of MPF (for discharges of the COD type). We shall study below the characteristics of the generation of AWs in developed optical discharges (ODs) of different types in connection with the possibility of remote acoustic diagnostics of ODs.

5. DIAGNOSTICS OF DISCHARGES OF THE TYPE LONG LASER SPARK

The specific nature of discharges of the LLS type is manifested at the later stages, when MPFs emerge into the surrounding gas and expand in it, as a rule, by the PDW mechanism. The comparatively low-frequency weakly damped components of the AWHs arising in this case under the conditions of dispersion and dissipation are the main source of acoustic information about the LLS in remote detection. The optical breakdown is characterized by the highest coefficient of conversion of the incident laser energy into acoustic energy; in contrast to traditional methods of optoacoustic laser spectroscopy,[31] this makes it possible to record the acoustic response directly in the free atmosphere. Since an LLS is characterized by several substantially different spatial scales, including the size of the plasma focus and the average distance between neighboring plasma foci, we shall distinguish the low-frequency components associated with them and we shall call them AWH_1 and AWH_2, respectively.

The following empirical relations exist[13]:

$$d_{PF} \simeq 0.71 \tau_+ v_s; \tag{2}$$

$$d_{PF} \simeq \frac{P_{p_+} r}{2100} \simeq \frac{P_{p_-} r}{1750}. \tag{3}$$

A remote microphone records the acoustic pulse generated by a separate plasma focus as a weak shock wave having the typical profile:[13] $\tau_- \simeq 1.5\tau_+$, $P_{p^+} \simeq 1.2 P_{p^-}$.

The relations (2) and (3) show that, like a source of sound, a separate plasma focus can be modelled as a pulsating sphere and its acoustic energy can be represented in the form

$$W_{PF} = \frac{4\pi r^2}{\rho_a v_s} \left(P_{p+}^2 \frac{\tau_+}{2} + P_{p-}^2 \frac{\tau_-}{2} \right). \tag{4}$$

The following notation was employed above: τ_+, τ_-, P_{p^+}, and P_{p^-} are the width (at the base) and peak pressures in the positive and negative phases, respectively, of the acoustic pulse generated by the plasma focus and r is the distance from the plasma focus to the receiving microphone.

Since the motion of the breakdown plasma along the laser beam for microsecond laser pulses occurs by the PDW mechanism, the change in the radius of the front of the shock wave, forming in the process, satisfies the relations of L.I. Sedov.[32] Then it is easy to show that for a square laser pulse the following relation is satisfied:

$$W_{1.p} \simeq \frac{\pi \cdot \rho_a d_{PF}^5}{12 \cdot \tau_1^2}, \tag{5}$$

where $W_{1.p}$ is the laser energy absorbed by the plasma focus. Assuming that a separate plasma focus almost completely absorbs the laser radiation incident on the body, we obtain from Eq. (4)

$$W_{PF} \simeq 3.1 \cdot 10^{-2} W_{1.p}^{2/5} \cdot d_{PF}. \tag{6}$$

Then the conversion factor for conversion of laser energy into acoustic energy is of the order of $K = W_{PF}/W_{1.p} \simeq 10^{-4}$, $W_{PF} \simeq E_1^{2/3}$.

The estimates presented above make it possible to interpret the result of the measurement of the parameters of the $AWH_{1,2}$ for the investigation of the nonlinear energy losses of the laser beam on the propagation path.[13] In particular, using the relation (2), the size of separate plasma foci can be determined by measuring τ_+, which in the frequency do-

main is equivalent to measuring the frequency corresponding to the maximum of the AWH_1 spectrum. The relation (3) makes it possible to determine, by measuring the amplitude of the AWH_1, the sizes of separate plasma foci and their size distribution. Figure 5 shows such a distribution for the laser source employed in the measurements. With the help of the measurements of the time delays between AWH_1 from each plasma focus with a known arrangement of the receiving microphone relative to the laser beam it is possible to reconstruct the spatial location of each plasma focus formed (Fig. 6). The traditional methods of spectral analysis permit finding from the AWH_2 spectrum the average distance between separate plasma foci and the size of the entire breakdown region.

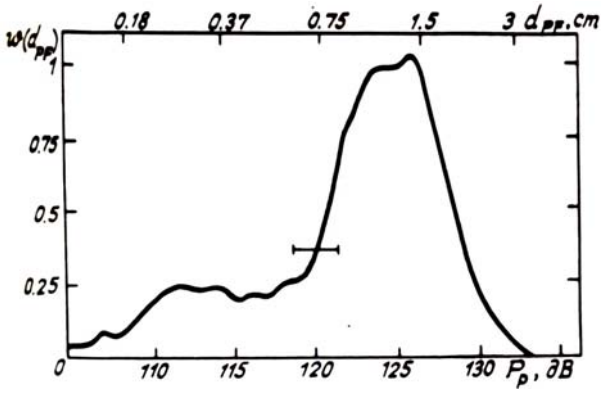

FIG. 5. The normalized size distribution function $w(d_{PF})$of the breakdown foci.

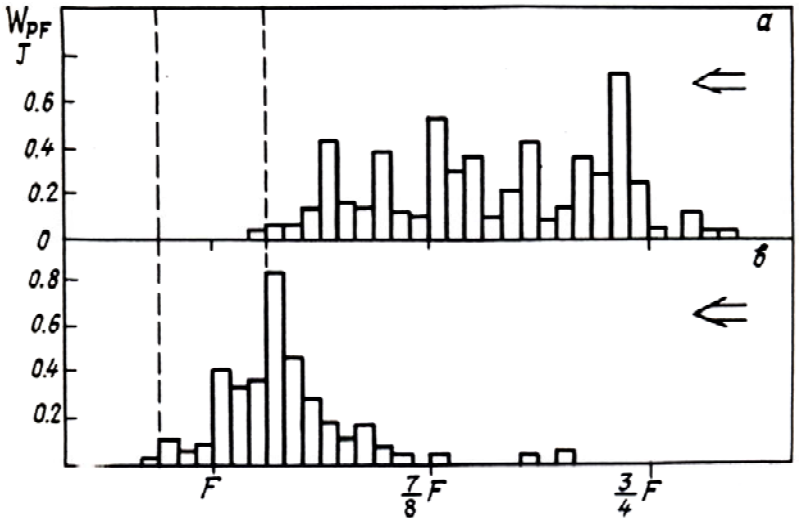

FIG. 6. Histograms of the running values o; the acoustic energy W generated along the propagation path of the laser beam a — $<n_a> = 33$ cm^{-3} and b — $<n_a> = 6$ cm^{-3}. The dashed lines show the region of the caustic of the laser beam and the arrows mark the direction of propagation.

6. GENERATION OF ACOUSTIC DISTURBANCES UNDER CONDITIONS OF COLLECTIVE INTERACTION IN DENSE AERODISPERSED SYSTEMS

The discharges of the LLS type studied above have in common the fact that the MPFs forming on the aerosol particles are only a seed that initiates the processes responsible for the propagation of the discharge into the buffer gas, which occur by the same mechanisms that are characteristic for single-phase systems and which result in the formation of the experimentally recorded plasma foci. A fundamentally different possibility of formation of plasma foci with sizes of the order of the focal volume appears in dense aerodispersed systems, when VAAs arising on separate particles can coalesce before the initiating pulse terminates. Such a collective process results in a sharp reduction of the thermal losses in the system and growth of the MPFs under conditions of anomalously low intensities, i.e., it can lead to the development of low-threshold COD. Depending on the ratio of the parameters of the problem the collective process can proceed along one of two basic channels[33]: 1) individual collective heating (ICH), when the MPFs develop in a self-maintained regime (see Sec. 4) and coalesce at a temperature much higher than the boiling point of the aerosol T_b; 2) cold coalescence (CC),[34] when MPFs do not form at all (see Sec. 2) and the heating is of a purely collective character (CH) and proceeds only after the VAAs coalesce at $T \simeq T_c$ owing to the sharp reduction of the relative thermal losses. In contrast to discharges of the LLS type the plasma focus of a COD forms and develops only in a two-component vapor-air medium, and the lowest threshold of breakdown should be expected (in the field of sufficiently wide pulses) precisely in the CC regime. We shall study the characteristics of AWs formed under these conditions.

In the aerosol ensemble characteristic for the formation of COD with sufficiently high aerosol concentration n_a the generation of an AWF on separate particles results in the formation of an acoustic wave connected with the merging of density and plasma waves

from separate VAAs. Following Ref. 20, this interference AWF can be called an acoustic wave of cold coalescence of the first type ($AWCC_1$). Its frequency range f_{AWCC_1} is determined by the transit time of the AWF in the cold buffer gas with velocity v_s between neighboring VAAs and thus can be estimated as

$$f_{AWCC_1} \sim v_s n_a^{1/3}. \tag{7}$$

One can see from Eq. (7) that the spectral interval of the $AWCC_1$ in an aerosol ensemble with concentration $n_a \sim 10^2$–10^4 cm^{-3} typical for a COD is hypersonic and lies in the region $f_{AFCC_1} \sim (1-6)\cdot 10^5$ Hz. The physical process of interference of AWFs, resulting in the formation of $AWCC_1$, can be investigated using the same mathematical model as that employed in Sec. 2 but supplemented with symmetric boundary conditions at the interface between two neighboring cells of the ensemble[18]:

$$\frac{\partial T}{\partial r} = 0, \quad v = 0, \quad \frac{\partial \rho_{a,b}}{\partial r} = 0,$$
$$t \in [0, \infty), \quad r = (4\pi n_a/3)^{-1/3}. \tag{8}$$

where v is the local velocity of the mixture of air and aerosol and ρ_a is the aerosol density.

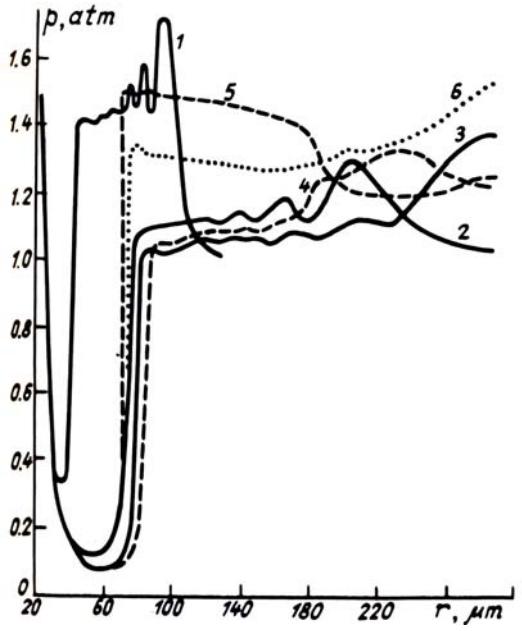

FIG. 7. The dynamics of the internal $AWCC_1$ in an ensemble of corundum aerosol particles ($a = 20$ μm, $\alpha = 5\cdot 10^3$ cm^{-3}) with concentration $n_a = 10^4$ cm^{-3} with intensity $I = 4\cdot 10^6$ W/cm^2 at successive times (μsec): 0.3 *(1),* 0.7 *(2),* 1.0 *(3),* 1.3 *(4),* 1.6 *(5), and* 2.1 *(6). The dashed lines are the pressure profiles after the first "reflection" from the interface of two neighboring cells and the dotted line is the profile after reflection from the region near the particle.*

The results of the calculations of the dynamics of the internal $AWCC_1$ are presented in Fig. 7, whence, in particular, one can see that the developed internal $AWCC_1$ has a frequency of the order of 1 MHz, in agreement with the estimate following from Eq. (7), and decays rapidly. The characteristic decay time, estimated from the results of numerical modeling, is $\tau_{CC} \sim 7$ μsec, which corresponds to an effective absorption coefficient $\alpha_{CC} \sim 5$ cm^{-1}. The fact that $\alpha_{CC} \gg \alpha_S$ for AWF at comparable frequencies (see Sec. 2) agrees with the well-known fact that in two-phase systems acoustic and shock waves are strongly damped (see, for example. Ref. 35).

The emergence of the $AWCC_1$ outside the generation zone is accompanied by transformation of the spectrum in the low-frequency region, where the absorption coefficient $\alpha_s \sim f^2$ is much smaller. However the strong dissipation of $AWCC_1$ in the HF region and the comparatively short generation time of acoustic waves of this type generated by the entire aerosol region ($\Delta t_1 \sim \min\{R_0/v_s, L_a/v_s\}$, where R_0 is the radius of the focal waist of the beam and L_a is the size of the aerosol cloud with a concentration of the order of n_a), makes it impossible to obtain from the $AWCC_1$ significant information about the discharge under conditions of remote detection. The total power of the $AWCC_1$ at distances $r \gg \min\{R_0, L_a\}$ must be of the same order of magnitude as in the case of generation of acoustic waves in the subthreshold regime.

If the COD develops in the CC regime, a signal associated with the coalescence of waves of heating (with $T \simeq T_c$) from separate VAAs is also generated in the system with some delay relative to the $AWCC_1$. We shall call the corresponding wave an acoustic wave of cold coalescence of the second type ($AWCC_2$). Since the wave of heating propagates with a much lower velocity than the AWF ($v_T \sim 10^3$ cm/sec $\ll v_S$), the spectral interval of the $AWCC_2$ for typical values of the concentration of the aerosol in the COD Is shifted into the acoustic range:

$$f_{AWCC_2} \sim v_T n_a^{1/3} \sim 5\cdot 10^3 - 2\cdot 10^4 \text{ Hz}. \tag{9}$$

As is obvious from Eq. (9),the $AWCC_2$ hardly decays, its total generation time is $\Delta t_2 \sim \min\{R_0/v_T, L_a/v_T\} \gg \Delta t_1$, and in the near-threshold regime of the COD this mechanism can be an effective source of AWs, recorded at a significant distance.

Under substantially above-threshold conditions for COD, when the system evolves in the ICH regime, an interference AWH is generated immediately after the $AWCC_1$. We shall call this wave an acoustic wave of collective heating of the first type ($AWCH_1$). The frequency spectrum of $AWCH_1$ lies in the same frequency interval as $AWCC_1$, while the delay time is determined by the conditions of heating and can range over wide limits. The results of numerical modeling of AWHs with high intensities give the lower limit (see Sec. 4). The upper limit

($\Delta t \sim 0.3$ msec) is obtained by shadow diagnostics of COD at intensities that are approximately two orders of magnitude lower.[18]

As in the case of cold coalescence, in the ICH regime a signal connected with the coalescence of heating fronts (with temperature much higher than T_c) from separate MPFs is generated in the system. We shall call the corresponding AWs, which has a frequency spectrum in the same interval as $AWCC_2$, an acoustic wave of collective heating of the second type ($AWCH_2$). As is obvious from what was said above, the $AWCH_2$ is the main form of AWs, recorded at a significant distance $r \gg \{R_0, L_a\}$ from the region of the COD under above-threshold conditions in the high-frequency part of the acoustic range. According to a number of indicators, the AW recorded in Ref. 17 at a distance $r \simeq 2$ cm from the region of the COD in the band $f \sim 10$ kHz with amplitude $\Delta P \simeq 0.04$ atm can be interpreted precisely as a $AWCH_2$.

Under threshold conditions of COD[36] an $AWCC_2$ is primarily recorded in the case of remote detection in the high-frequency part of the acoustic range (since it is precisely the CC–CH mechanism that gives the lowest threshold). It should be kept in mind, however, that a powerful AW, connected with heating and expansion of the region of the COD as a single plasma focus, forms at the CH stage. We shall call this wave an acoustic wave of collective heating of the third type ($AWCH_3$). Its frequency interval

$$f_{AWCH_3} \sim v_\perp / 4\pi \min\{R_0, L_a\} \qquad (10)$$

can be estimated, in principle, in the same way as for AWH_1, generated by a separate plasma focus in discharges of the LLS type (see Sec. 5). The quantitative differences are connected, first of all, with the fact that Eq. (10) contains the rate of expansion of the COD across the beam (based on data from the shadow and holographic diagnostics[37,38] $v_\perp = 15$–70 m/sec $< v_S$) and, second, with the fact that the characteristic size of the plasma focus in discharges of the LLS type is, as a rule, smaller than the size of the COD. As a result for beams with $R_0 \sim 0.2$–3 cm we have $f_{AWCH_3} = 40$ Hz – 3 kHz. It is obvious that a wave of the type $AWCH_3$, only more powerful, will also be generated in the substantially above-threshold regimes of ICH, since the discharge passes through the CH stage in this case also. Thus the $AWCH_3$ is the lowest frequency component of acoustic waves from the region of the COD and is the most reliable indicator of the emergence of the discharge into the collective regime both under threshold conditions and significantly above the breakdown threshold.

The possibility of acoustic diagnostics of the threshold conditions of COD was demonstrated in a laboratory experiment.[20]

The details of the structure of the spectra of AWs vary from one realization to another for identical (within the limits of accuracy of the measurements) experimental conditions. However the character of the spectra as a whole obeys completely determinate laws, which can be traced based on the theoretical model constructed above for the generation of AWs and the energy threshold of COD[33,34,36]:

$$\pi a^2 n_a I \tau_L = Q \geq Q^*, \qquad (11)$$

where Q^* is a threshold parameter that depends primarily on the aerosol material and the external pressure. For boron carbide (B_4C) and a pressure $P = 1$ atm $Q^* = 130$ J/cm^2.[33]

The main feature revealed by the analysis of the spectra of the acoustic signals from the region of COD is the possibility of direct diagnostics of CC and CH processes based on data obtained by remote acoustic detection in the acoustic range. Diagnostics of hypersonic AWs of the type AWF, AWH, $AWCC_1$, and $AWCH_1$ cannot, however, be performed as reliably as for low-frequency AWs of the type $AWCC_2$, $AWCH_2$, and $AWCH_3$.

Comparing the spectra measured with increasing values of the parameter Q makes it possible to follow the increase in the relative input of acoustic energy by the CH process. The separation of a low-frequency maximum in the acoustic spectrum of COD can be used as a criterion for satisfying the threshold condition (11), relating the parameters of the aerodispersed system (a, n_a) and the laser pulse. When an independent channel for measuring one of the parameters of the aerosol is available, the second parameter can be determined from Eq. (11). One method of remote estimation of n_a could also be based on spectral analysis of AWs, namely, determination of the maxima of $AWCC_2$ or $AWCH_2$ and using the relation (9).

8. CONSLUSIONS

Aerodispersed systems at atmospheric pressure in the field of powerful near- and far-IR laser radiation are efficient sources of AWs in a wide spectral interval, under both below-threshold and especially above-threshold conditions for development of optical discharges of different types. The generalized scheme of laser generation of AWs, which makes it possible to classify the waves, is presented in Fig. 8 in a symbolic form.

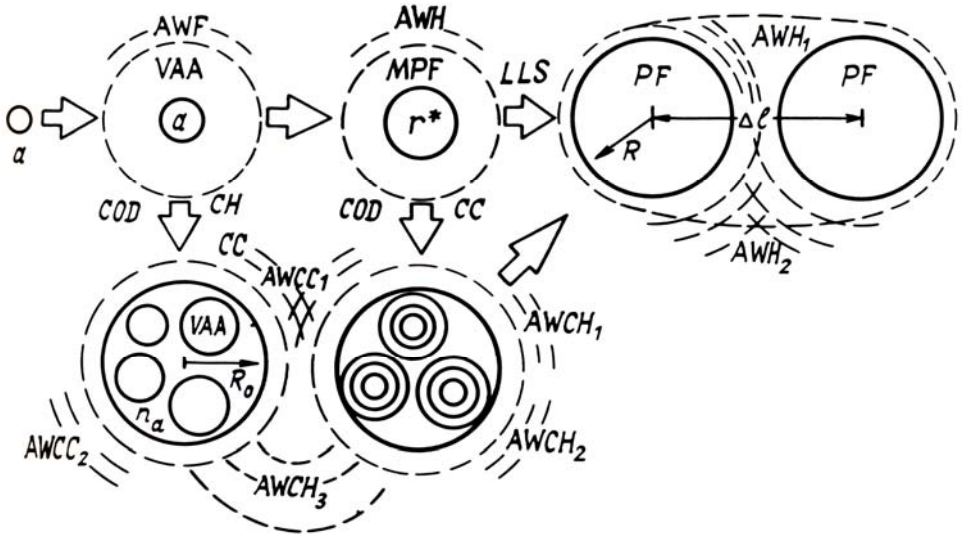

FIG. 8. Generalized scheme of laser generation of acoustic waves in aerosols.

Depending on the regime of interaction of laser radiation with the aerosol the following components of the AWs can form:

1) a near-field hypersonic acoustic wave of formation of a microflame (AWF) with a rapidly transformed (over a time 10^{-7}—10^{-6} sec) spectrum (10^8 Hz > f_{AWF} > 10^6 Hz) both below and above threshold for COD. and distant acoustic AWF with a spectrum right down to 20 Hz;

2) near—field hypersonic acoustic wave of heating (AWH) of the microflame, whose frequency interval depends strongly on the intensity (10^7 Hz > f_{AWF} > 10^5 Hz) — above threshold for LLS and substantially above threshold for COD, and remote acoustic AWH_1 and AWH_2 in discharges of the LLS type;

3) acoustic waves of cold coalescence in different types of COD: at first hypersonic waves ($AWCC_1$) with frequencies of the order of 10^5 Hz and then at near-threshold conditions acoustic waves ($AWCC_2$) with frequencies $5 \cdot 10^3$—$2 \cdot 10^4$ Hz; the frequency of the AWCC depends on the aerosol concentration; and,

4) acoustic waves of collective heating (AWCH) in discharges of the type COD, both hypersonic ($AWCH_1$) and high-frequency acoustic ($AWCH_2$) far above threshold and low-frequency acoustic ($AWCH_3$) at the stage of developed COD above threshold.

The acoustic waves generated can not only be the product of the optical discharge, but they can also affect the dynamics of the discharge. For intensities characteristic for LLS at distances not greater than the range of propagation of a photodetonation wave r_{PD1} or the decay length of AWH $r_{AWH} < \alpha_{AWH}^{-1} \simeq 1.6$ cm, the plasma foci can interact with one smother, but not in the form of collective heating, like in COD, but rather in the form of competition[39]: in a sufficiently close ensemble of stronger (developing earlier) plasma foci a neighboring plasma focus, located at a distance Δr, is extinguished if its development time exceeds

$$t^* = \begin{cases} \Delta r / v_{PDW}, & \Delta r < r_{PDW}, \\ \Delta r / v_s, & r_{PDW} < \Delta r < r_{AWH}. \end{cases}$$

Remote measurements of the integrated energy of acoustic waves in the acoustic range give an estimate of the energy of the beam or the total aerosol content. Spectral processing of acoustic waves carries significant information about the structure and dynamics of the region of interaction of powerful laser radiation with the aerosol both below and above threshold. In addition, as the frequency of the received and processed acoustic waves increases, diagnostics of smaller spatial and time intervals can be performed. In the case of wide laser pulses with comparatively low intensity it is of great practical interest to perform diagnostics of slow collective processes occurring in am aerosol whose concentration is high. Effective diagnostics of such processes can be performed in the acoustic range. In this case the low-frequency maximum of the acoustic spectrum carries information about the transverse size of the region of the discharge and the higher frequency maxima carry information about the character of the spatial distribution of the aerosol particles. In particular, from the ratio of the indicated maxima it is possible to determine whether or not the threshold condition for COD is satisfied.

REFERENCES

1. L.M. Lyamshev, Usp. Fiz. Nauk **151**, No. 3, 479—527 (1987).
2. V.E. Zuev, *Propagation of Laser Radiation in the Atmosphere* [in Russian], Radio i Svyaz', Moscow (1981), 287 pp.

3. Yu.D. Kopytin and L.G. Shamanaeva, in: *Abstracts of Reports at the 8th All-Union Symposium on the Propagation of Laser Radiation in the Atmosphere,* Tomsk Affiliate of the Siberian Branch of the Academy of Sciences of the USSR, Tomsk (1986), Part 2. pp. 319–328.
4. N.N. Bochkarev, Yu.D. Kopytln, N.P. Krasnenko, et al., ibid., pp. 216–220.
5. G.A. Askar'yan, A.M. Prokhorov, G.F. Chanturiya, and G.P. Shipulo, Zh. Eksp. Teor. Fiz. **44**, No. 6, 2180–2185 (1963).
6. N.N. Bochkarev, N.P. Krasnenko, V.A. Pogodaev, and A.E. Rozhdestvenskii, in: *Abstracts of Reports at the 2nd All-Union Symposium on the Propagation of Laser Radiation in a Dispersed Medium*, Obninsk (1985), Part 4, pp. 42–45.
7. N.N. Bochkarev, A.A. Zemlyanov, N.P. Krasnenko, et al., Pis'ma Zh. Tekh. Fiz. **14**, No. 1, 25–29 (1988).
8. N.N. Bochkarev, Yu.E. Geints, A.A. Zemlyanov, et al., Opt. Atmos. **1**, No. 10, 111–112 (1988).
9. E.B. Belyaev, A.P. Godlevskii, Yu.D. Kopytin, et al., in: *Abstracts of Reports at the 2nd Conference on Atmospheric Optics*, Institute of Atmospheric Optics of the Siberian Branch of the Academy of Sciences of the USSR. Tomsk (1980), Part 3, pp. 156–159.
10. E.B. Belyaev. A.P. Godlevskii, Yu.D. Kopytin, et al., Pis'ma Zh. Tekh. Fiz. **8**, No. 8, 333–337 (1982).
11. Yu.V. Akhtyrchenko, N.N. Bochkarev, Yu.P. Visotsky, et al., in: *Abstracts of Reports at the 8th All-Union Symposium on Laser and Acoustic Atmosphere Sounding*, Tomsk Affiliate of the Siberian Branch of the Academy of Sciences of the USSR, Tomsk (1984), Part 2, pp. 114–118.
12. V.E. Zuev, V.P. Muravskii, V.L. S'edin, and L.G. Shamanaeva, ibid., pp. 119–123.
13. N.N. Bochkarev, Yu.D. Kopytin, N.P. Krasnenko, et al., in: *Abstracts of Reports at the 8th All-Union Symposium on the Propagation of Laser Radiation in the Atmosphere,* Tomsk Affiliate of the Siberian Branch of the Academy of Sciences of the USSR. Tomsk (1986), Part 2, pp. 194–198.
14. R.A. Baikalova, G.M. Krekov, V.P. Muravskii, and L.G. Shamanaeva, in: *Abstracts of Reports at the 9th All-Union Symposium on Laser and Acoustic Sounding of the Atmosphere*, Tomsk Affiliate of the Siberian Branch of the Academy of Sciences of the USSR, Tomsk (1987), Part 1. pp. 468–472.
15. Yu.E. Geints, A.A. Zemlyanov, A.M. Kabanov, et al., ibid., pp. 397–402.
16. I.Ya. Korolev, Yu.M. Sorokin, and A.M. Cheremukhin, in*: Abstracts of Reports at the 7th All-UnionSymposium on the Propagation of Laser Radiation in the Atmosphere*, Tomsk Affiliate of the Siberian Branch of the Academy of Sciences of the USSR, Tomsk (1983), pp. 153–154.
17. V.I. Bukatyi, A.A. Kobolov, and A.A. Tel'nikhin, Zh. Tekh. Fiz. **55**, No. 2, 312–318 (1985).
18. I.Ya. Korolev, T.P. Kosoburd, V.A. Vdovin, and Yu.M. Sorokin, Zh. Tekh. Fiz. **57**, No. 12, 2314–2323 (1987).
19. V.A. Vdovin and Yu.M. Sorokin, *"The dynamics of the formation of an aerosol microflame accompanying low-threshold optical breakdown"*, VINITI, No. 7038-V87 S«pt. 30, 1987, (1987).
20. I.Ya. Korolev, A.V. Samokhvalov, and Yu.M. Sorokin, Opt. Atmos. **1**, No. 1, 73–80 (1988).
21. Yu.P. Raizer, *The Laser Spark and the Propagation of Discharges* [in Russian], Nauka, Moscow (1974), 308 pp.
22. S.V. Zakharchenko, S.D. Pinchuk, and A.M. Skripkin, Kvant. Elektron. **5**, No. 4, 934–937 (1978).
23. A.D. Surridge, Acustica **44**, No. 3, 207 (1980).
24. A.A. Samokhin, *The Effect of a Laser Beam on Absorbing and Condensed Media* [in Russian], Tr. IOFAN, Nauka, Moscow (1988), Vol. 13, pp. 3–98.
25. Yu.E. Geints, and A.A. Zemlyanov. *"The propagation of laser radiation under conditions of explosive break-up of absorbing particles of water aerosol,"* VINITI, No. 3658-V88, May 12, 1988, 45 pp.
26. Yu.E. Geints, A.A. Zemlyanov, V.A. Pogodaev, and A.E. Rozhdestvenskii, Opt. Atmos. **1**, No. 3, 27–34 (1988).
27. F.V. Bunkin and V.V. Savranskii, Zh. Exp. Teor. Fiz. **65**, No. 6, 2185–2195 (1973).
28. A.M. Skripkin, Zh. Tekh. Fiz. **57**, No. 3, 554–556 (1987).
29. R.G. Pinnick, P. Chylek, M. Tarzembski, et al., Appl. Optics **27**, No. 5, 987 (1988).
30. P. Chylek, M.A. Tarzembski, V. Srivastava, et al., Appl. Optics **26**, No. 5, 760 (1987).
31. V.P. Zharov and V.S. Letokhov, *Laser Optoacoustic Spectroscopy* [in Russian], Nauka, Moscow (1984), 320 pp.
32. L.I. Sedov, *Similarity and Dimension Methods in Mechanics* [in Russian], Nauka, Moscow (1972), 440 pp.
33. Yu.M. Sorokin, I.Ya. Korolev, and E.M. Krikunova, Kvant. Elektron. **13**, No. 12, 2464–2473 (1986).
34. Yu.M. Sorokin. Zh. Tekh. Fiz. **56**, No. 7, 1431–1433 (1986).
35. T.P. Gavrilenko, and V.V. Grigor'ev, Fiz. Goreniya Vzryva **20**, No. 1, 86–90 (1984).
36. Yu.M. Sorokin, Opt. Atmos. **1**, No. 8, 36–43 (1988).
37. T.P. Kosoburd, and Yu.M. Sorokin, Zh. Tekh. Fiz. **58**, No. 7, 1318–1324 (1988).
38. Yu.N. Zakharov and Yu.M. Sorokin, Atmos. Opt. **2**, No. 2. 140 (1989).
39. S.V. Zakharchenko, A.M. Skripkin. Zh. Tekh. Fiz. **55**, No. 10, 1935–1942 (1985).